
On a Recoverability of Graph Neural Network Representations

Maxim Fishman*
Technion, Habana Labs

Chaim Baskin*
Technion
chaimbaskin@cs.technion.ac.il

Evgenii Zheltonozhskii*
Technion

Almog David
Technion

Ron Banner
Habana Labs

Avi Mendelson
Technion

Abstract

Despite their growing popularity, graph neural networks (GNNs) still have multiple unsolved problems, including lack of embedding expressiveness, propagation of information to distant nodes, and training on large-scale graphs. Understanding the roots of and providing solutions for such problems require developing analytic tools and techniques. In this work, we propose the notion of *recoverability*, which measures the amount of information contained in a random variable for being able to recover another one from it. We provide a method for an efficient empirical estimation of recoverability, demonstrate a tight relationship of it to information aggregation in GNNs, and show how this new concept can be used in unsupervised graph representation learning. We demonstrate, through extensive experimental results on various datasets and different GNN architectures, that estimated recoverability correlates with aggregation method expressivity and graph sparsification quality, the GNN representations can be learned using our unsupervised approach, and the recoverability regularization can mitigate accuracy drop caused by expanding of GNN depth. The code to reproduce our experiments is available at <https://github.com/Anonymous1252022/Recoverability>.

1 Introduction

Over the last decade, deep learning allowed researchers to tackle multiple hard tasks, previously considered intractable. For example, convolutional neural networks (CNNs) have been successfully applied to computer vision problems such as image classification [He et al., 2016], object detection [Ren et al., 2015], and semantic segmentation [Ronneberger et al., 2015]. Nevertheless, while CNNs are successful in processing pixels, multiple other modalities such as 3D meshes [Wu et al., 2019], social networks [Ribeiro et al., 2017], brain connections [Shapson-Coe et al., 2021], relational databases [Cvitkovic, 2020], citation graphs [Sen et al., 2008], sensor networks [Bloemheuvel et al., 2021] and many others, require the processing of irregular data. As a result, in recent years, researchers have been looking into ways to exploit deep learning methods, such as CNNs, in order to work with graph structured data. Deep learning on graphs and, in particular, Graph Neural Networks [GNNs, Gori et al., 2005, Scarselli et al., 2008, Kipf and Welling, 2017], based on message passing [Gilmer et al., 2017], i.e., iterative updating of a graph node representation based on information aggregated from its neighbors, have become a very popular tool for machine learning with graphs.

Even though GNNs show exceptional ability to learn graph-based data representations, there are still some unsolved problems limiting their performance. One issue is related to aggregation method

*Equal contribution.

expressiveness. [Kipf and Welling \[2017\]](#) proposed graph convolution networks (GCNs), which aggregate information from neighboring nodes but cannot distinguish between them. To solve this problem, [Veličković et al. \[2018\]](#) integrated a self-attention mechanism [[Vaswani et al., 2017](#)] into aggregation, proposing graph attention networks (GAT). Another problem is lack of ability to propagate information between distant nodes in the graph. [Li et al. \[2018\]](#) conjectured that this phenomenon is a result of *over-smoothing*, a situation in which node representations become indistinguishable when the number of layers increases. [Alon and Yahav \[2021\]](#) offered another explanation – *over-squashing* of an exponentially growing amount of information into fixed-size vectors. Finally, training on large-scale graphs is a significant obstacle in integrating GNNs in real-life problems. In real-life graphs, the diameter (maximal distance between two nodes) is often small (3–5) even for large graphs. Thus, GCNs with only 3–5 layers must aggregate information from the whole graph to calculate embedding of a single node, which requires a large amount of memory and compute, and also causes a *bottleneck* [[Alon and Yahav, 2021](#)]. One way to reduce the amount of computation is to use sampling techniques such as SAGE [[Hamilton et al., 2017](#)] or SAINT [[Zeng et al., 2020](#)]. Another way is to sparsify the graph by dropping a subset of edges [[Srinivasa et al., 2020](#), [Rathee et al., 2021](#)].

In this work, we introduce the notion of *recoverability* and demonstrate its tight relationship to information aggregation in GNNs. Recoverability provides an alternative insight into the aforementioned problems and can serve as a good tool for understanding their roots and finding solutions for them. First, we define a recoverability loss and provide an efficient and differentiable way of its estimation via reproducing kernel Hilbert space (RKHS) embedding. Then, we demonstrate how the recoverability can be used in the node property prediction tasks, and provide a case study algorithm for illustrating the principle of how to use the recoverability in unsupervised graph representation learning. Finally, we present an extensive experimental results on various datasets and different GNN architectures.

Our main contributions are as follows:

- We define a notion of recoverability along with an efficient and differentiable method of its estimation (in contrast to similar notion of mutual information, which is hard to estimate).
- We provide a method for GNN embedding analysis and show how the recoverability can be used in unsupervised setting.
- We provide experimental results to empirically confirm the efficiency of recoverability for GNN embedding analysis and unsupervised graph representation learning.

2 Related Work

In our work, we demonstrate an embedding method analysis based on the amount of information aggregated in the GNN embedding. The proposed approach is somewhat similar to Usable Information [[Kleinman et al., 2021](#)], a notion based on entropy estimation. However, [Kleinman et al. \[2021\]](#) did not consider GNN architectures, and the entropy estimation from the samples is challenging in high-dimensional setting. A few works that utilize information-theoretic tools in GNNs already exist. One popular approach is to maximize mutual information (MI) [[Peng et al., 2020](#), [Bandyopadhyay et al., 2020](#), [Sun et al., 2020](#)] for learning better graph representations both in supervised and unsupervised settings. In those works, MI is estimated via MINE [[Belghazi et al., 2018](#)] or its improvement, MI-NEE [[Chan et al., 2019](#)], which involve a lot of additional parameters that should be learned for correct MI estimation.

We eliminate MI estimation in our work by turning to functional analytic tools. We define recoverability and use RKHS [[Aronszajn, 1950](#)] embedding, a popular approach in machine learning toolbox [[Hofmann et al., 2008](#), [Muandet et al., 2017](#), [Klebanov et al., 2021](#)], with a universal kernel [[Micchelli et al., 2006](#)] for its estimation. As a result, while recoverability has some similarity with MI, it is less challenging for estimation, since there is no need to involve additional learnable parameters. In addition, similar to [Peng et al. \[2020\]](#), we use recoverability loss minimization (instead of MI maximization) for graph representation learning in unsupervised setting. In the context of bias-variance decomposition [[Geman et al., 1992](#), [Domingos, 2000](#), [Yang et al., 2020](#)], recoverability measures the amount of noise in the loss.

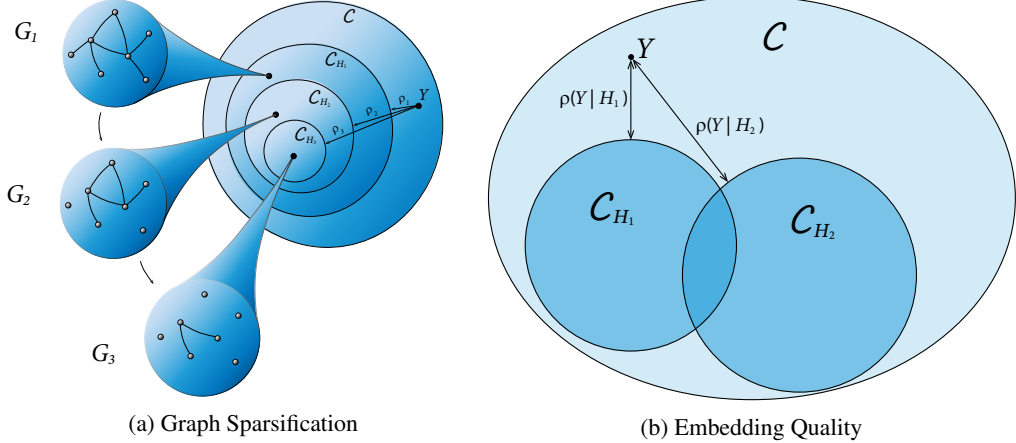


Figure 1: **(a)** The relation between graph sparsification and recoverability loss. G_2 and G_3 are sparsified versions of graph G_1 , and Y is the node class random variable. The fewer edges there are in G_i , the smaller the corresponding space \mathcal{C}_{H_i} , and, consequently, recoverability loss ρ is higher. **(b)** H_1 and H_2 are two embeddings of the same graph. The distance $\rho(Y|H_1)$ is smaller than $\rho(Y|H_2)$, and thus Y is better recoverable from H_1 than from H_2 , i.e. the embedding H_1 is better than H_2 .

3 Recoverability of Graph Representations

In the following sections we introduce the notion of recoverability, which is tightly related to useful information contained in one random variable for being able to recover another random variable from it. In Theorem 1 we show that RKHS embedding can be used for efficient recoverability loss estimation from given samples. In addition, in the context of node property prediction tasks, we demonstrate how recoverability can be used for measuring the quality of a given embedding method. Finally, we demonstrate, providing case study algorithm, how to use recoverability in unsupervised learning of graph representations.

3.1 Recoverability

Given two random variables X and Y , with the values in \mathbb{R}^m and \mathbb{R}^n , respectively, we say that Y is fully recoverable from X if there exists a continuous map $f : \mathbb{R}^m \rightarrow \mathbb{R}^n$ such that $f(X) = Y$. However, we do not necessarily have such a relation between X and Y , which means that we cannot fully recover Y from X . Nevertheless, X may still contain some information from which we can partially recover Y . To measure the amount of such information in X , we define

$$\mathcal{C}_X = \{f(X) \mid f : \mathbb{R}^m \rightarrow \mathbb{R}^n \text{ is continuous function}\}, \quad (1)$$

i.e., the collection of all random variables that could be fully recovered from X , and evaluate the distance between random variable Y and the set \mathcal{C}_X :

$$\rho(Y|X) = \inf_{Z \in \mathcal{C}_X} d(Y, Z) \quad (2)$$

where d is some distance function. We call the quantity $\rho(Y|X)$ *recoverability loss*.

Let $\rho^*(Y|X)$ be empirical estimation of $\rho(Y|X)$ on a finite collection of samples $(x, y) = \{(x_k, y_k)\}_{k \in [N]}$, where L_p -norm is used for measuring the distance between two random variables for $p \in [1, \infty)$.

Theorem 1 Let $K_{ij} = \exp\left(-\frac{\|x_i - x_j\|^2}{2\sigma^2}\right)$ be a Gram matrix, and Π be an orthogonal projection onto the $\text{Im}(K)$. The empirical estimation of L_p -recoverability loss is given by

$$\rho^*(Y|X) = \frac{1}{n} \sum_{i \in [n]} \frac{1}{N^{1/p}} \left\| (\mathbb{I} - \Pi) y^{(i)} \right\|_p. \quad (3)$$

We provide the proof of the Theorem 1 in Appendix A. In Appendix B we demonstrate the connection between recoverability loss minimization and mutual information maximization, and show that both have similar effect on random variables although the recoverability estimation from samples is less challenging for high-dimensional random variables than the mutual information estimation.

3.2 Recoverability in Node Property Prediction Task

In the node property prediction task, given graph $G = (V, E)$ equipped with node features $\mathcal{X} = \{x_v\}_{v \in V}$ and labels $\mathcal{Y} = \{y_v\}_{v \in V}$ distributed according to some probability distribution $(x_v, y_v) \sim (X, Y)$, one should predict the label of each node in the graph. For embedding method analysis, we chose to use the model consisting of two consecutive blocks, where the first block is an embedding, composed of k consecutive graph convolution layers, and the second block is a classifier acting on individual nodes. The purpose of the first block is to aggregate the information from the neighbourhood, whereas the second block is some continuous (not necessarily linear) map from the node embeddings (the output of the first block) to the node classes.

The model first embeds the graph with node features (G, \mathcal{X}) into a latent space, acquiring some representation of each node, which we denote $h_v \sim H$, and then apply a classifier to the embedding h_v , trying to predict label y_v . The success of the above procedure is highly dependent on the ability to learn a map between random variables H and Y . Since different embedding methods produce different random variables, we can reduce the problem of measuring the embedding method's quality to measuring the ability to learn random variable Y from random variable H , i.e. estimating the recoverability loss $\rho(Y|H)$: lower recoverability loss indicates the quality of the embedding method is higher. Assume we have two embedding methods EM_1 and EM_2 , which produce two different random variables H_1 and H_2 , respectively, as visualized in Fig. 1b. The distance between Y and C_{H_1} is smaller than between Y and C_{H_2} , meaning that Y is less recoverable from H_2 than from H_1 . In other words, embedding method EM_1 aggregates more information for recovering Y , than EM_2 .

Same idea can be used in the graph sparsification. In the Fig. 1a we can see three graphs G_1 , G_2 , and G_3 ; G_2 and G_3 are sparser versions of G_1 . Same embedding method applied to different graphs produces different random variables, H_1 , H_2 , and H_3 , respectively. Since we expect that dropping the edges reduces the amount of relevant information in the embeddings, the distance of random variable Y from the sets C_{H_2} and C_{H_3} should be larger than the distance from C_{H_1} , as illustrated in Fig. 1a. However, in some cases, the edges in the graph may bring no additional information, or even be harmful due to their noisy nature (with respect to adjacent node features). Removing those edges may decrease the recoverability loss. This concept can be used for measuring the quality of a given sparsification method or even finding the better one.

3.3 Recoverability in Graph Unsupervised Learning

In unsupervised representation learning our goal is to learn some meaningful representation of the nodes without using any labels, in contrast to the node property prediction task. Without labels, it is a priori unknown which information should be preserved in the node embedding to succeed in the downstream task. In this case, we prefer to keep as much information as it possible in the extracted features.

For a single GNN layer (Fig. 2), let X be a random variable distributed as input node features and Z be a random variable distributed as neighbouring node features, i.e., $Z|X = x_i$ is a uniform mixture of neighbours of nodes with features x_i . Finally, let H be a random variable distributed as output node features (node embedding of a single GNN layer). The random variable H contains full information about random variables X and Z , if there exist continuous maps f and g such that $f(H) = X$ and $g(H) = Z$. In this case we have $\rho(X|H) + \rho(Z|H) = 0$. Thus, in Algorithm 1 we minimize common recoverability loss $\rho(X|H) + \rho(Z|H)$ for all the layers in the GNN.

4 Experiments

The information about datasets used in our experiments is summarized in Table D.2.

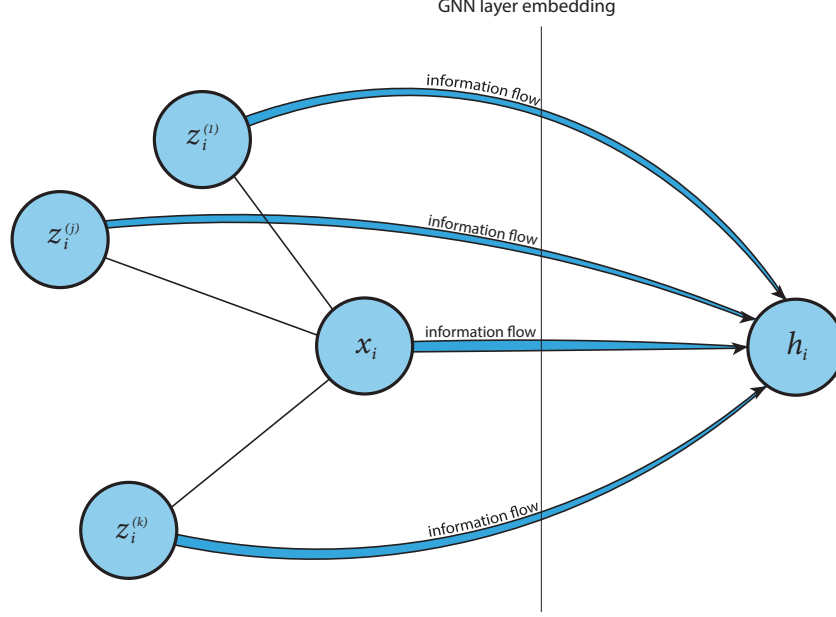


Figure 2: A single GNN layer, where the vertical line separates the input features from the output features. x_i is vector of input node features, $z_i^{(j)}$, for $j \in [k]$, are vectors of neighboring nodes features and h_i is vector of output node features. During $\rho(X|H) + \rho(Z|H)$ minimization, h_i aggregates information from x_i and all $z_i^{(j)}$.

Algorithm 1 Unsupervised Graph Representation Learning

```

Input:  $(G, \{x_n\}_{n \in [N]})$ , GNN
Output: GNN
for batch  $I \subseteq N$  do
    for layer  $l \in [d]$  do
         $\{h_i^{(l)}\}_{i \in I} \leftarrow GNN_l(G, \{h_i^{(l-1)}\}_{i \in I})$  single layer embedding, where  $h_i^{(0)} = x_i$ 
        for  $i \in I$  do
             $z_i^{(l-1)} \leftarrow h_j^{(l-1)}$ , where  $j$  is uniformly sampled from  $N(i)$ 
        end for
         $\rho_l \leftarrow \rho^*(H^{(l-1)}|H^{(l)}) + \rho^*(Z^{(l-1)}|H^{(l)})$ 
    end for
     $\rho \leftarrow \sum_{l \in [d]} \rho_l$ 
    apply SGD step to minimize  $\rho$ 
end for

```

Throughout the experiments we use five different embedding layers²: GCNConv [Kipf and Welling, 2017], SAGEConv [Hamilton et al., 2017], GINConv [Xu et al., 2019], GraphConv [Morris et al., 2019], and GATv2Conv [Brody et al., 2022]. More details on those embedding layers are given in Appendix E.

For all experiments, except Section 4.5, the GNN model consists of two consecutive blocks, where the first block is an embedding built from k graph convolutional layers, and the second block is a classifier composed of three fully connected layers. Each layer in the model except for the last one is followed by ReLU activation and dropout. The GNN model for unsupervised graph representation learning is described in Section 4.5.

All experiments were executed on Nvidia RTX A6000 GPUs.

²The notation is taken from PyTorch Geometric [Fey and Lenssen, 2019].

	Reddit2	ogbn-arxiv	Flickr	PPI	ogbn-products
$\rho^*(Y X)$	0.088	0.085	0.188	0.374	0.041
$\rho^*(Y H)$	0.066	0.079	0.183	0.287	0.017
$\Delta\rho$	25%	7%	2.3%	23%	58.5%
Homophily	0.782	0.654	0.319	0.620 [†]	0.808

Table 1: The recoverability loss before ($\rho^*(Y|X)$) and after ($\rho^*(Y|H)$) application of embedding method aggregation to the input node features. Recoverability loss ρ decreases when the embedding method aggregation is applied to the node features ($\rho^*(Y|H) < \rho^*(Y|X)$). $\Delta\rho$ is the recoverability loss relative drop. An interesting correlation is observed between recoverability loss drop and dataset homophily. [†] The homophily of PPI is the average over all classes.

4.1 The Usefulness of Edges

The first experiment shows an interesting property of the datasets appearing in Table D.2, which could help elucidate why GNNs with a SAGEConv layer can be used efficiently for training on these. We took three consecutive SAGEConv layers without learnable parameters as embedding method EM, i.e., only the aggregation parts, and applied it to the node features. Let X denote the random variable of node features, H the node embedding (after EM application) and Y the node classes. From Table 1 we can see that $\rho^*(Y|H) < \rho^*(Y|X)$. In other words, Y is more recoverable from H (node embedding) than from X (node features). Additionally, we observe an interesting correlation between recoverability loss drop and homophily. In the Reddit2 and ogbn-products datasets, which have a relatively high homophily, the recoverability loss drops relatively sharply, whereas in the Flickr dataset, which has a relatively low homophily, the recoverability loss changes relatively slightly.

4.2 Correlation Between Recoverability and Aggregation Method Quality

In this experiment we demonstrate the correlation between recoverability loss and aggregation method quality on a given dataset, measured with the test accuracy after the training on a GNN model defined in Section 4. For GraphConv, GCNConv, SAGEConv and GINConv, the estimation of recoverability loss was done only on the aggregation part of the embedding, i.e. all learnable parameters were dropped. For GATv2Conv, the recoverability loss was computed for the node embedding of the trained model.

The results are shown in Fig. 3. The plots for the rest datasets are given in Appendix F.1. While dropping learnable parameters is a significant simplification that does not fully capture expressive power of GNNs, we still observe a strong correlation between recoverability and the test accuracy for all datasets, allowing to compare the quality of the different approaches without training the network.

4.3 Propagation of Information to Distant Nodes

Here, we demonstrate the depth problem in GNNs, its correlation with the recoverability, and the ability to mitigate this issue through recoverability loss regularization. We trained two GNN models with three and nine SAGEConv layers (the model architecture is defined in Section 4) on datasets from Table D.2. In addition, we trained nine-layer network with recoverability regularization added to loss, i.e. $\mathcal{L}_{total} = \mathcal{L} + \lambda (\sum_i \rho^*(Y|H_i))$, where \mathcal{L} is the original training loss, λ – regularization parameter, and H_i – outputs of each SAGEConv layer. The results are summarized in Table 2. For the Reddit2, ogbn-arxiv and ogbn-products datasets, we did not see a significant change in test accuracy after depth expansion, whereas for the Flickr and PPI datasets, there was a degradation in accuracy for nine-layer architecture. We collected the recoverability loss of each embedding layer in the trained nine-layer architecture. The results are shown in Fig. 4. To make the trend more notable, we merged all plots and omitted the recoverability loss values. For Reddit2, ogbn-arxiv and ogbn-products, we have a similar pattern of ρ behavior: it smoothly decreases, meaning that each consecutive layer aggregates more and more information to recover Y . For Flickr and PPI, we see different behavior. In Flickr, ρ increases, indicating that it does not aggregate any useful information from neighboring nodes to recover Y . In PPI, ρ first decreases and starts to increase after three layers, which indicates that the *over-smoothing* [Li et al., 2018] or *over-squashing* [Alon and Yahav, 2021] problem is

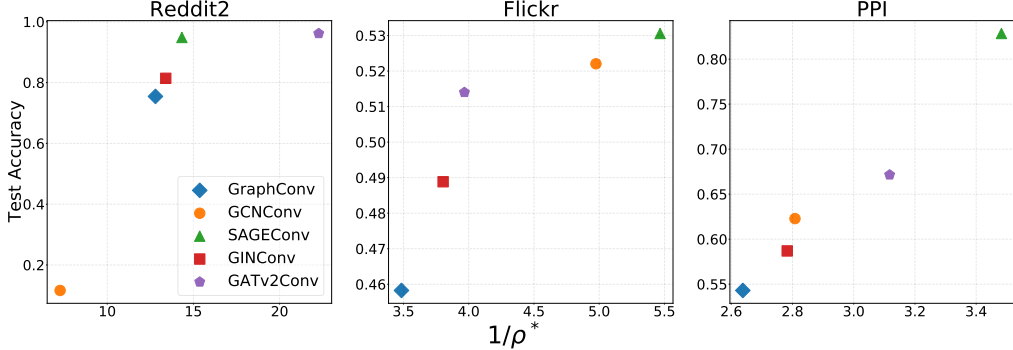


Figure 3: Correlation between the recoverability loss and the aggregation method quality for the chosen datasets, i.e., the test accuracy after the training on GNN models. The y -axis is the test accuracy of the trained GNN model on a given dataset, and the x -axis is the inverse of the estimated recoverability loss ($1/\rho^*$). For GraphConv, GCNConv, SAGEConv and GINConv, the estimation of recoverability loss was done only on the aggregation part of the embedding, like in Table 1. For GATv2Conv, the recoverability loss was computed for the node embedding of the trained model. As the recoverability loss drops, the test accuracy becomes higher.

Depth	Regularized	Accuracy				
		Reddit2	ogbn-arxiv	ogbn-products	Flickr	PPI
3	–	0.946 ± 0.002	0.692 ± 0.002	0.789 ± 0.0004	0.532 ± 0.001	0.831 ± 0.003
9	–	0.943 ± 0.006	0.691 ± 0.009	0.792 ± 0.0006	0.522 ± 0.004	0.761 ± 0.002
9	✓	0.962 ± 0.001	0.695 ± 0.003	0.796 ± 0.003	0.538 ± 0.003	0.797 ± 0.001

Table 2: Test accuracy of trained models with three and nine SAGEConv layers, with and without the recoverability regularization was used during the training. For Flickr and PPI datasets there is an accuracy degradation when number of layers is increased to nine. This degradation is mitigated through recoverability regularization both for Flickr and significantly reduced for PPI.

occurring. In addition, one can see that the accuracy drop for Flickr and PPI datasets was mitigated when recoverability regularization was used during the training.

4.4 Correlation Between Recoverability and the Graph Sparsification Method Quality

In this experiment we show that the quality of the given sparsification method correlates with recoverability. We use two simple sparsification methods. In **Random** sparsification we randomly drop 90% of the edges from the graph. In **Max d** sparsification we find the maximal value of d that satisfies $\sum_{v \in V} \min\{d, d_{\text{in}}(v)\} \leq 0.1|E|$, where $d_{\text{in}}(v)$ is an input degree of v , and $|E|$ is the number of edges in the graph. Then, for each node v in the graph we randomly leave $\min\{d, d_{\text{in}}(v)\}$ of input edges. Both methods leave 10% of the edges in the graph.

To evaluate quality of sparsification, we first apply it to the given dataset and then train a three-layer SAGEConv GNN mode (defined in Section 4) on sparsified data. We also compute the recoverability loss of the aggregation part of embedding, i.e. without learnable parameters. The results are shown in Table 3. We see that the **Max d** sparsification is better than **Random**, and correspondingly, the recoverability loss of **Max d** is lower than that of **Random**.

4.5 GNN Unsupervised Learning Using Recoverability

The last experiment demonstrates the effectiveness of using recoverability loss for information aggregation in unsupervised setting, where we tested the proposed algorithm (Section 3.3).

In this case, the embedding block is composed of k graph convolutional layers followed by ELU activation. The classifier, used in downstream task, consists of two fully connected layers with ELU

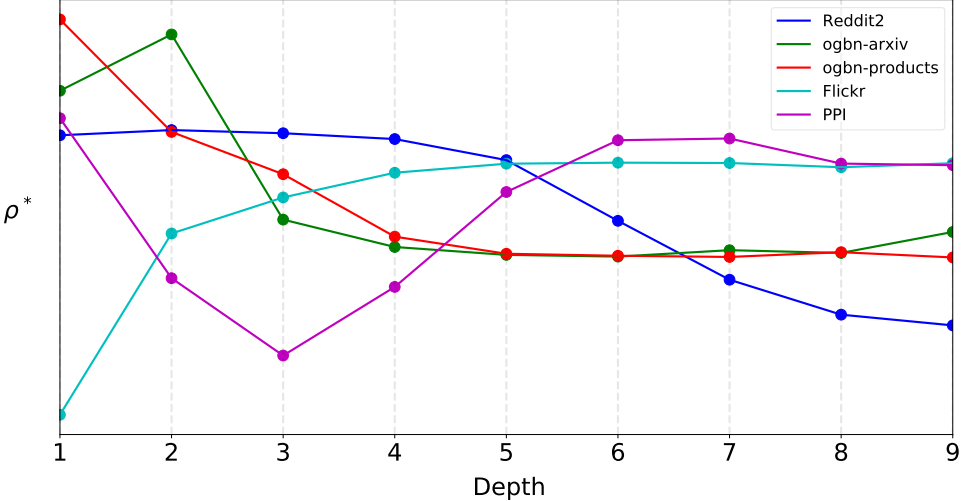


Figure 4: The recoverability loss of each embedding layer in trained nine-layer GNN model. The recoverability of the Flickr and PPI datasets behaves differently than the recoverability of the Reddit2, ogbn-arxiv and ogbn-products datasets. Note the correlation with second row in Table 2.

		Reddit2	ogbn-arxiv	Flickr	PPI	ogbn-products
Random	ρ	0.083	0.109	0.214	0.313	0.020
	Accuracy	0.906 ± 0.005	0.568 ± 0.007	0.466 ± 0.001	0.598 ± 0.001	0.705 ± 0.002
Max d	ρ	0.069	0.084	0.191	0.266	0.017
	Accuracy	0.938 ± 0.005	0.586 ± 0.004	0.470 ± 0.004	0.617 ± 0.001	0.767 ± 0.002

Table 3: Comparison of two simple sparsification methods, “Random” and “Max d” with 90% of the edges dropped from the graphs. There is a noticeable correlation between recoverability loss and test accuracy.

activation between them. In supervised setting, same blocks (embedding and classifier) are used with batch norm added between each graph convolution layer and ELU activation.

The results with GCNConv and GATConv layers are summarized in Fig. 5, where two rows correspond to two different layer types. The plots for the rest datasets are given in Appendix F.2. We compare test accuracy of our unsupervised approach with supervised version, simple MLP and current supervised state-of-the-art [Wan et al., 2022, Chien et al., 2021, Zhao et al., 2021]. To evaluate test accuracy of unsupervised setting, the embedding was first learned using Algorithm 1, then classifier was trained on frozen features.

While the baseline models are not achieving state-of-the-art performance in supervised settings, our unsupervised model significantly outperforms MLP baseline, achieving accuracy close to supervised baseline. In addition, we see that in many cases additional aggregation layers improve performance, demonstrating successful information aggregation from the neighbouring nodes.

We compare our unsupervised graph representation learning algorithm (Algorithm 1), with GMI-mean [Peng et al., 2020], an unsupervised graph representation learning algorithm which is based on MI maximization in Table 4. We tuned number of layers and layer type for each dataset, acquiring best results with four GCNConv layers for Reddit2, three SAGEConv layers for PPI, and four GATConv for PubMed. The results suggest that our recoverability metric can be used for unsupervised learning, demonstrating encouraging results compared to existing methods based on MI maximization, and, in some cases (such as PPI), even outperforming them.

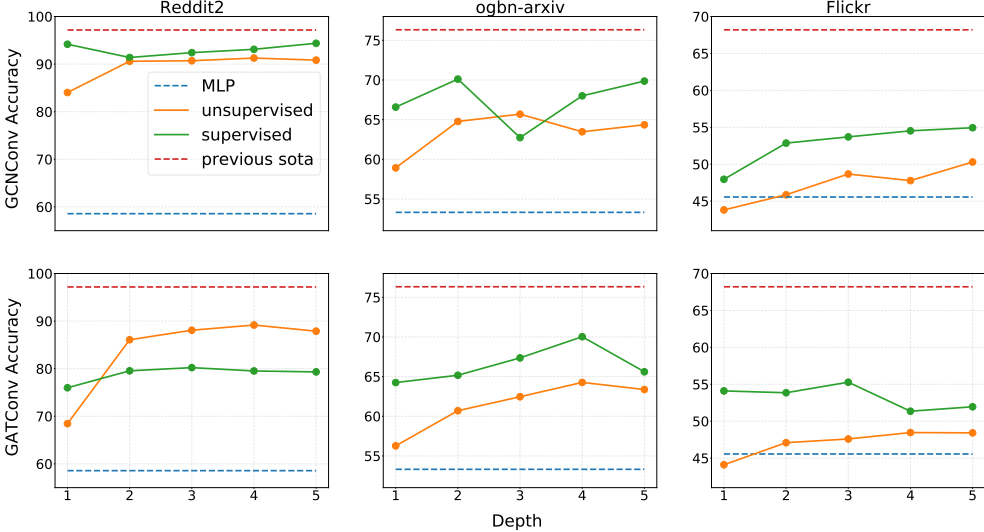


Figure 5: GNN unsupervised learning using recoverability. Each column refers to different dataset. Each row corresponds to different graph convolution layer type. Each plot consists of test accuracy for supervised/unsupervised settings, MLP accuracy and previous supervised sota accuracy.

Method	Accuracy		
	Reddit2	PPI	PubMed
GMI-mean [Peng et al., 2020]	95.0 \pm 0.02	65.0 \pm 0.02	80.1 \pm 0.2
Ours	91.27 \pm 0.34	97.31 \pm 0.19	78.12 \pm 2.34

Table 4: The comparison between our recoverability loss (Algorithm 1) and MI maximization for unsupervised graph representation learning.

5 Discussion

We introduced a notion of recoverability, which has similarity with mutual information, but, by virtue of RKHS embedding with universal kernel, does not require additional learnable parameters and thus is less challenging for estimation from samples in high-dimensional settings.

We demonstrated multiple applications of the recoverability both for analysis and training of GNNs: it allows us to quantify the usefulness of edges in the node classification tasks and compare different graph embedding methods.

The recoverability can be used as a loss term, minimization of which can lead to higher prediction accuracy, especially for deep GNNs. In Section 4.3, recoverability regularization improved accuracy for Flickr and PPI in nine-layer architecture, and even outperformed three-layer architecture for Reddit2.

We demonstrated how recoverability can be used in unsupervised setting, providing an algorithm for graph representation learning. This can potentially replace MI-based losses in unsupervised graph representation learning, resulting in more computationally efficient training. The results in Section 4.5 reveal the trend of information aggregation using provided algorithm.

In overall, the notion of recoverability could provide an essential tool for understanding the roots of and providing better solutions for the problems with GNNs, such as the expressiveness of the aggregation method, propagation of information to distant nodes and training on large-scale graphs.

References

Uri Alon and Eran Yahav. On the bottleneck of graph neural networks and its practical implications. In *International Conference on Learning Representations*, 2021. URL <https://openreview.net/forum?id=i800Ph0CVH2>. (cited on pp. 2 and 6)

Nachman Aronszajn. Theory of reproducing kernels. *Transactions of the American mathematical society*, 68(3):337–404, 1950. (cited on p. 2)

Sambaran Bandyopadhyay, Manasvi Aggarwal, and M. Narasimha Murty. Unsupervised graph representation by periphery and hierarchical information maximization. *arXiv preprint arXiv:2006.04696*, 2020. URL <https://arxiv.org/abs/2006.04696>. (cited on p. 2)

Mohamed Ishmael Belghazi, Aristide Baratin, Sai Rajeswar, Sherjil Ozair, Yoshua Bengio, Aaron Courville, and R Devon Hjelm. MINE: mutual information neural estimation. *arXiv preprint arXiv:1801.04062*, 2018. URL <https://arxiv.org/abs/1801.04062>. (cited on p. 2)

Stefan Bloemheuvel, Jurgen van den Hoogen, and Martin Atzmueller. A computational framework for modeling complex sensor network data using graph signal processing and graph neural networks in structural health monitoring. *arXiv preprint arXiv:2105.05316*, 2021. (cited on p. 1)

Shaked Brody, Uri Alon, and Eran Yahav. How attentive are graph attention networks? In *International Conference on Learning Representations*, 2022. URL <https://openreview.net/forum?id=F72ximsx7C1>. (cited on p. 5)

Chung Chan, Ali Al-Bashabsheh, Hing Pang Huang, Michael Lim, Da Sun Handason Tam, and Chao Zhao. Neural entropic estimation: A faster path to mutual information estimation. 2019. (cited on p. 2)

Eli Chien, Wei-Cheng Chang, Cho-Jui Hsieh, Hsiang-Fu Yu, Jiong Zhang, Olgica Milenkovic, and Inderjit S. Dhillon. Node feature extraction by self-supervised multi-scale neighborhood prediction. *arXiv preprint arXiv:2111.00064*, 2021. (cited on p. 8)

Milan Cvitkovic. Supervised learning on relational databases with graph neural networks. *arXiv preprint arXiv:2002.02046*, 2020. (cited on p. 1)

Pedro Domingos. A unified bias-variance decomposition and its applications. In *Proceedings of the Seventeenth International Conference on Machine Learning*, ICML '00, page 231–238, San Francisco, CA, USA, 2000. Morgan Kaufmann Publishers Inc. ISBN 1558607072. (cited on p. 2)

Matthias Fey and Jan Eric Lenssen. Fast graph representation learning with pytorch geometric. 2019. URL https://github.com/pyg-team/pytorch_geometric. (cited on p. 5)

Stuart Geman, Elie Bienenstock, and René Doursat. Neural Networks and the Bias/Variance Dilemma. *Neural Computation*, 4(1):1–58, 01 1992. ISSN 0899-7667. doi: 10.1162/neco.1992.4.1.1. URL <https://doi.org/10.1162/neco.1992.4.1.1>. (cited on p. 2)

Justin Gilmer, Samuel S. Schoenholz, Patrick F. Riley, Oriol Vinyals, and George E. Dahl. Neural message passing for quantum chemistry. In Doina Precup and Yee Whye Teh, editors, *Proceedings of the 34th International Conference on Machine Learning*, volume 70 of *Proceedings of Machine Learning Research*, pages 1263–1272. PMLR, 06–11 Aug 2017. URL <https://proceedings.mlr.press/v70/gilmer17a.html>. (cited on p. 1)

Marco Gori, Gabriele Monfardini, and Franco Scarselli. A new model for learning in graph domains. In *Proceedings. 2005 IEEE International Joint Conference on Neural Networks, 2005.*, volume 2, pages 729–734. IEEE, 2005. (cited on p. 1)

Will Hamilton, Zhitao Ying, and Jure Leskovec. Inductive representation learning on large graphs. In I. Guyon, U. V. Luxburg, S. Bengio, H. Wallach, R. Fergus, S. Vishwanathan, and R. Garnett, editors, *Advances in Neural Information Processing Systems*, volume 30. Curran Associates, Inc., 2017. URL <https://proceedings.neurips.cc/paper/2017/hash/5dd9db5e033da9c6fb5ba83c7a7ebea9-Abstract.html>. (cited on pp. 2, 5, and 18)

Kaiming He, Xiangyu Zhang, Shaoqing Ren, and Jian Sun. Deep residual learning for image recognition. In *Proceedings of the IEEE Conference on Computer Vision and Pattern Recognition (CVPR)*, June 2016. URL https://www.cv-foundation.org/openaccess/content_cvpr_2016/html/He_Deep_Residual_Learning_CVPR_2016_paper.html. (cited on p. 1)

Thomas Hofmann, Bernhard Schölkopf, and Alexander J. Smola. Kernel methods in machine learning. *The Annals of Statistics*, 36(3), Jun 2008. ISSN 0090-5364. doi: 10.1214/009053607000000677. URL <http://dx.doi.org/10.1214/009053607000000677>. (cited on p. 2)

Weihua Hu, Matthias Fey, Marinka Zitnik, Yuxiao Dong, Hongyu Ren, Bowen Liu, Michele Catasta, and Jure Leskovec. Open graph benchmark: Datasets for machine learning on graphs. In H. Larochelle, M. Ranzato, R. Hadsell, M. F. Balcan, and H. Lin, editors, *Advances in Neural Information Processing Systems*, volume 33, pages 22118–22133. Curran Associates, Inc., 2020. URL <https://proceedings.neurips.cc/paper/2020/hash/fb60d411a5c5b72b2e7d3527cfc84fd0-Abstract.html>. (cited on p. 18)

George S. Kimeldorf and Grace Wahba. A correspondence between Bayesian estimation on stochastic processes and smoothing by splines. *The Annals of Mathematical Statistics*, 41(2):495 – 502, 1970. doi: 10.1214/aoms/1177697089. URL <https://doi.org/10.1214/aoms/1177697089>. (cited on p. 14)

Thomas N. Kipf and Max Welling. Semi-supervised classification with graph convolutional networks. In *International Conference on Learning Representations*, 2017. URL <https://openreview.net/forum?id=SJU4ayYgl>. (cited on pp. 1, 2, and 5)

Ilja Klebanov, Björn Sprungk, and Tim J. Sullivan. The linear conditional expectation in Hilbert space. *Bernoulli*, 27(4):2267 – 2299, 2021. doi: 10.3150/20-BEJ1308. URL <https://doi.org/10.3150/20-BEJ1308>. (cited on p. 2)

Michael Kleinman, Alessandro Achille, Daksh Idnani, and Jonathan Kao. Usable information and evolution of optimal representations during training. In *International Conference on Learning Representations*, 2021. URL <https://openreview.net/forum?id=p8agn6bmTbr>. (cited on p. 2)

Qimai Li, Zhichao Han, and Xiao-Ming Wu. Deeper insights into graph convolutional networks for semi-supervised learning. *Proceedings of the AAAI Conference on Artificial Intelligence*, 32(1), Apr. 2018. URL <https://ojs.aaai.org/index.php/AAAI/article/view/11604>. (cited on pp. 2 and 6)

Charles A. Micchelli, Yuesheng Xu, and Haizhang Zhang. Universal kernels. *Journal of Machine Learning Research*, 7(95):2651–2667, 2006. URL <http://jmlr.org/papers/v7/micchelli06a.html>. (cited on pp. 2 and 14)

Christopher Morris, Martin Ritzert, Matthias Fey, William L. Hamilton, Jan Eric Lenssen, Gaurav Rattan, and Martin Grohe. Weisfeiler and Leman go neural: Higher-order graph neural networks. *Proceedings of the AAAI Conference on Artificial Intelligence*, 33(01):4602–4609, Jul. 2019. doi: 10.1609/aaai.v33i01.33014602. URL <https://ojs.aaai.org/index.php/AAAI/article/view/4384>. (cited on p. 5)

Krikamol Muandet, Kenji Fukumizu, Bharath Sriperumbudur, and Bernhard Schölkopf. Kernel mean embedding of distributions: A review and beyond. *Foundations and Trends® in Machine Learning*, 10(1-2):1–141, 2017. ISSN 1935-8245. doi: 10.1561/2200000060. URL <http://dx.doi.org/10.1561/2200000060>. (cited on p. 2)

Zhen Peng, Wenbing Huang, Minnan Luo, Qinghua Zheng, Yu Rong, Tingyang Xu, and Junzhou Huang. Graph representation learning via graphical mutual information maximization. In *Proceedings of The Web Conference 2020*, page 259–270, New York, NY, USA, 2020. Association for Computing Machinery. ISBN 9781450370233. URL <https://doi.org/10.1145/3366423.3380112>. (cited on pp. 2, 8, and 9)

Mandeep Rathee, Zijian Zhang, Thorben Funke, Megha Khosla, and Avishek Anand. Learnt sparsification for interpretable graph neural networks. *arXiv preprint arXiv:2106.12920*, 2021. URL <https://arxiv.org/abs/2106.12920>. (cited on p. 2)

Shaoqing Ren, Kaiming He, Ross Girshick, and Jian Sun. Faster R-CNN: Towards real-time object detection with region proposal networks. In C. Cortes, N. Lawrence, D. Lee, M. Sugiyama, and R. Garnett, editors, *Advances in Neural Information Processing Systems*, volume 28. Curran Associates, Inc., 2015. URL <https://proceedings.neurips.cc/paper/2015/hash/14bfa6bb14875e45bba028a21ed38046-Abstract.html>. (cited on p. 1)

Manoel Horta Ribeiro, Pedro H. Calais, Yuri A. Santos, Virgílio A. F. Almeida, and Wagner Meira Jr. “Like sheep among wolves”: Characterizing hateful users on twitter. *arXiv preprint arXiv:1801.00317*, 2017. (cited on p. 1)

Olaf Ronneberger, Philipp Fischer, and Thomas Brox. U-net: Convolutional networks for biomedical image segmentation. In *International Conference on Medical image computing and computer-assisted intervention*, pages 234–241. Springer, 2015. (cited on p. 1)

Franco Scarselli, Marco Gori, Ah Chung Tsoi, Markus Hagenbuchner, and Gabriele Monfardini. The graph neural network model. *IEEE transactions on neural networks*, 20(1):61–80, 2008. (cited on p. 1)

Prithviraj Sen, Galileo Namata, Mustafa Bilgic, Lise Getoor, Brian Galligher, and Tina Eliassi-Rad. Collective classification in network data. *AI Magazine*, 29(3):93, Sep. 2008. (cited on p. 1)

Alexander Shapson-Coe, Michał Januszewski, Daniel R. Berger, Art Pope, Yuelong Wu, Tim Blakely, Richard L. Schalek, Peter Li, Shuhong Wang, Jeremy Maitin-Shepard, Neha Karlupia, Sven Dorkenwald, Evelina Sjostedt, Laramie Leavitt, Dongil Lee, Luke Bailey, Angerica Fitzmaurice, Rohin Kar, Benjamin Field, Hank Wu, Julian Wagner-Carena, David Aley, Joanna Lau, Zudi Lin, Donglai Wei, Hanspeter Pfister, Adi Peleg, Viren Jain, and Jeff W. Lichtman. A connectomic study of a petascale fragment of human cerebral cortex. *bioRxiv*, 2021. doi: 10.1101/2021.05.29.446289. URL <https://www.biorxiv.org/content/early/2021/05/30/2021.05.29.446289>. (cited on p. 1)

Rakshit S Srinivasa, Cao Xiao, Lucas Glass, Justin Romberg, and Jimeng Sun. Fast graph attention networks using effective resistance based graph sparsification. 2020. (cited on p. 2)

Fan-Yun Sun, Jordan Hoffman, Vikas Verma, and Jian Tang. InfoGraph: unsupervised and semi-supervised graph-level representation learning via mutual information maximization. In *International Conference on Learning Representations*, 2020. URL <https://openreview.net/forum?id=r11fF2NYvH>. (cited on p. 2)

Ashish Vaswani, Noam Shazeer, Niki Parmar, Jakob Uszkoreit, Llion Jones, Aidan N. Gomez, Łukasz Kaiser, and Illia Polosukhin. Attention is all you need. In I. Guyon, U. V. Luxburg, S. Bengio, H. Wallach, R. Fergus, S. Vishwanathan, and R. Garnett, editors, *Advances in Neural Information Processing Systems*, volume 30. Curran Associates, Inc., 2017. URL <https://proceedings.neurips.cc/paper/2017/hash/3f5ee243547dee91fb053c1c4a845aa-Abstract.html>. (cited on p. 2)

Petar Veličković, Guillem Cucurull, Arantxa Casanova, Adriana Romero, Pietro Liò, and Yoshua Bengio. Graph attention networks. In *International Conference on Learning Representations*, 2018. URL <https://openreview.net/forum?id=rJXMpikCZ>. (cited on p. 2)

Cheng Wan, Youjie Li, Ang Li, Nam Sung Kim, and Yingyan Lin. Bns-gen: Efficient full-graph training of graph convolutional networks with partition-parallelism and random boundary node sampling. *Proceedings of Machine Learning and Systems*, 4, 2022. (cited on p. 8)

Zizhao Wu, Ming Zeng, Feiwei Qin, Yigang Wang, and Jiří Kosinka. Active 3-d shape cosegmentation with graph convolutional networks. *IEEE computer graphics and applications*, 39(2):77–88, 2019. (cited on p. 1)

Keyulu Xu, Weihua Hu, Jure Leskovec, and Stefanie Jegelka. How powerful are graph neural networks? In *International Conference on Learning Representations*, 2019. URL <https://openreview.net/forum?id=ryGs6iA5Km>. (cited on p. 5)

Zhilin Yang, William W. Cohen, and Ruslan Salakhutdinov. Revisiting semi-supervised learning with graph embeddings. 2016. doi: 10.48550/ARXIV.1603.08861. URL <https://arxiv.org/abs/1603.08861>. (cited on p. 18)

Zitong Yang, Yaodong Yu, Chong You, Jacob Steinhardt, and Yi Ma. Rethinking bias-variance trade-off for generalization of neural networks. In Hal Daumé III and Aarti Singh, editors, *Proceedings of the 37th International Conference on Machine Learning*, volume 119 of *Proceedings of Machine Learning Research*, pages 10767–10777. PMLR, 13–18 Jul 2020. URL <https://proceedings.mlr.press/v119/yang20j.html>. (cited on p. 2)

Hanqing Zeng, Hongkuan Zhou, Ajitesh Srivastava, Rajgopal Kannan, and Viktor Prasanna. Graph-SAINT: graph sampling based inductive learning method. In *International Conference on Learning Representations*, 2020. URL <https://openreview.net/forum?id=BJe8pkHFwS>. (cited on pp. 2 and 18)

Tong Zhao, Yozen Liu, Leonardo Neves, Oliver Woodford, Meng Jiang, and Neil Shah. Data augmentation for graph neural networks. *Proceedings of the AAAI Conference on Artificial Intelligence*, 35(12):11015–11023, May 2021. URL <https://ojs.aaai.org/index.php/AAAI/article/view/17315>. (cited on p. 8)

A Proof of Theorem 1

Let $U \subset \mathbb{R}^d$ be a compact³ set,

$$C(U) = \{f : U \rightarrow \mathbb{R} \mid f \text{ is continuous function}\}, \quad (\text{A.1})$$

and

$$\forall x_1, x_2 \in U \quad k(x_1, x_2) = \exp\left(-\frac{\|x_1 - x_2\|^2}{2\sigma^2}\right). \quad (\text{A.2})$$

For each $x \in U$, define continuous function $k(x, \cdot) = \phi_x(\cdot)$, and construct the following functional space:

$$\mathcal{H}_0 = \text{span}(\{\phi_x(\cdot) \mid \forall x \in U\}) \quad (\text{A.3})$$

Define an inner product on \mathcal{H}_0 as follows:

$$\left\langle \sum_{i=1}^n a_i \phi_{x_i}(\cdot), \sum_{j=1}^m b_j \phi_{x_j}(\cdot) \right\rangle = \sum_{i=1}^n \sum_{j=1}^m a_i b_j k(x_i, x_j) \quad (\text{A.4})$$

Let \mathcal{H} be the completion of \mathcal{H}_0 with respect to this inner product. Now \mathcal{H} is an RKHS built from the kernel $k(\cdot, \cdot)$.

Since $k(\cdot, \cdot)$ is a universal kernel [Micchelli et al., 2006], the set \mathcal{H} is dense in $C(U)$ with respect to the supremum norm, i.e.:

$$\forall f \in C(U) \quad \forall \epsilon > 0 \quad \exists g \in \mathcal{H} \text{ s.t. } \sup_{x \in U} |f(x) - g(x)| < \epsilon \quad (\text{A.5})$$

In addition, \mathcal{H} has reproducing property:

$$\forall f \in \mathcal{H} \quad \forall x \in U \quad f(x) = \langle f, \phi_x(\cdot) \rangle \quad (\text{A.6})$$

and thus we have:

$$\rho(Y^{(i)}|X) = \inf_{Z \in \mathcal{C}_X} d(Y^{(i)}, Z) = \inf_{f \in C(U)} d(Y^{(i)}, f(X)) = \quad (\text{A.7})$$

$$= \inf_{f \in \mathcal{H}} d(Y^{(i)}, f(X)) = \inf_{f \in \mathcal{H}} d(Y^{(i)}, \langle f, \phi_X(\cdot) \rangle) \quad (\text{A.8})$$

We denote the estimation of ρ on a finite collection of samples $(x, y) = \{(x_k, y_k)\}_{k \in [N]}$ by ρ^* and use the distance induced from L_p -norm, where $p \in [1, \infty)$. Thus we have:

$$\rho^*(Y^{(i)}|X) = \inf_{f \in \mathcal{H}} \left(\frac{1}{N} \sum_{k \in [N]} |y_k^{(i)} - \langle f, \phi_{x_k}(\cdot) \rangle|^p \right)^{1/p} \quad (\text{A.9})$$

From the *representer theorem* [Kimeldorf and Wahba, 1970] there exists $f^* \in \mathcal{H}$ of the following form:

$$f^* = \sum_{i \in [N]} \alpha_i \phi_{x_i}(\cdot) \quad (\text{A.10})$$

which minimizes $\rho^*(Y^{(i)}|X)$. Thus:

$$\rho^*(Y^{(i)}|X) = \left(\frac{1}{N} \sum_{k \in [N]} |y_k^{(i)} - \langle f^*, \phi_{x_k}(\cdot) \rangle|^p \right)^{1/p} = \quad (\text{A.11})$$

$$= \min_{\alpha_j \in \mathbb{R}} \left(\frac{1}{N} \sum_{k \in [N]} |y_k^{(i)} - \sum_{j \in [N]} \alpha_j k(h_i, h_j)|^p \right)^{1/p} = \min_{\alpha \in \mathbb{R}^N} \frac{1}{N^{1/p}} \|y^{(i)} - K\alpha\|_p \quad (\text{A.12})$$

³It is not a restrictive assumption that U is compact set since all tensor values in neural networks are bounded.

where $K_{ij} = k(x_i, x_j)$ is a Gram matrix.

Decompose $y^{(i)}$ into two parts:

$$y^{(i)} = y_{\parallel}^{(i)} + y_{\perp}^{(i)} \quad (\text{A.13})$$

where $y_{\parallel}^{(i)} \in \text{im}(K)$ and $\forall v \in \text{im}(K) \quad \left(y_{\perp}^{(i)}\right)^T v = 0$. Then we have:

$$\rho^*(Y^{(i)}|X) = \frac{1}{N^{1/p}} \left\| y_{\perp}^{(i)} \right\|_p \quad (\text{A.14})$$

Since K is positive semi-definite, we have the following eigendecomposition:

$$K = U \Lambda U^T \quad (\text{A.15})$$

where columns of unitary matrix U are eigenvectors of K and Λ is a diagonal matrix of eigenvalues. Let:

$$\lambda_1, \lambda_2, \dots, \lambda_k, 0, 0, \dots, 0 \quad (\text{A.16})$$

be the descending order of eigenvalues, where $\lambda_k > 0$. Then:

$$\Pi = \sum_{i \in [k]} u_i u_i^T \quad (\text{A.17})$$

is an orthogonal projection into $\text{im}(K)$ subspace. Consequently:

$$\rho^*(Y^{(i)}|X) = \frac{1}{N^{1/p}} \left\| (\mathbb{I} - \Pi) y^{(i)} \right\|_p \quad (\text{A.18})$$

where \mathbb{I} is an identity matrix. And thus, we have:

$$\rho^*(Y|X) = \frac{1}{n} \sum_{i \in [n]} \frac{1}{N^{1/p}} \left\| (\mathbb{I} - \Pi) y^{(i)} \right\|_p \quad (\text{A.19})$$

B The Recoverability Loss and the Mutual Information

This part is intended to answer two questions:

1. What is common between recoverability loss and mutual information?
2. Is the recoverability loss better than the mutual information?

The best way to understand the connection between the recoverability loss and the mutual information is through σ -algebras, the objects taken from measure theory. A σ -algebra \mathcal{A} is a collection of subsets of Ω where the following set of properties is satisfied:

1. $\emptyset \in \mathcal{A}$
2. $A \in \mathcal{A} \Rightarrow A^c \in \mathcal{A}$
3. $\{A_n\}_{n \in \mathbb{N}} \subseteq \mathcal{A} \Rightarrow \cup_{n \in \mathbb{N}} A_n \in \mathcal{A}$

Each random variable $X : \Omega \rightarrow \mathbb{R}$ has its own σ -algebra which is defined as follows:

$$\sigma_X = \{X^{-1}(A) : A \in \mathcal{B}(\mathbb{R})\} \quad (\text{B.20})$$

where $\mathcal{B}(\mathbb{R})$ is a Borel σ -algebra on \mathbb{R} .

The conventional definition of the entropy of the random variable X is given by expectation of negative logarithm of probability density function:

$$H(X) = \mathbb{E}[-\ln f_X(X)] \quad (\text{B.21})$$

The equivalent, measure theoretic, definition of the entropy $H(X)$ is:

$$H(\sigma_X) = \sup_{P \subseteq \sigma_X} \sum_{A \in P} -\mathbb{P}(A) \ln \mathbb{P}(A) \quad (\text{B.22})$$

where P is a \mathbb{P} -almost partition of Ω , i.e. satisfies the following:

1. $\mathbb{P}(\cup_{A \in P} A) = 1$
2. $\forall A, B \in P \quad \mathbb{P}(A \cap B) = 0$

From two aforementioned definitions we can conclude that the entropy is fully dependent only on a σ -algebra of a given random variable. Thus, σ -algebra can be interpreted as a sort of information contained in the random variable, and the entropy measures the amount of such information.

The mutual information between two random variable X and Y is defined as:

$$I(X; Y) = H(X) + H(Y) - H(X, Y) = H(\sigma_X) + H(\sigma_Y) - H(\sigma(\sigma_X \cup \sigma_Y)) \quad (\text{B.23})$$

Assuming that we change only random variable X , when we maximize the mutual information $I(X; Y)$ we have:

$$H(\sigma_X) = H(\sigma(\sigma_X \cup \sigma_Y)) \quad (\text{B.24})$$

what means:

$$\sigma_Y \subseteq \sigma_X \quad (\text{B.25})$$

On the other side, when we minimize the recoverability loss $\rho(Y|X)$ we have:

$$\exists f \text{ - a measurable function s.t. } f(X) = Y \quad (\text{B.26})$$

what again means:

$$\sigma_Y \subseteq \sigma_X \quad (\text{B.27})$$

In conclusion, by mutual information maximization and recoverability loss minimization, we do similar thing, make σ_Y to be sub-algebra of σ_X . The difference is that $I(X; Y)$ is symmetric with respect to X and Y , whereas $\rho(Y|X)$ is not.

However, the estimation of mutual information form samples is challenging for high-dimensional random variables. The main difficulty comes from estimation of high-dimensional probability density function from the given samples, since generally the number of samples required scales exponentially with the dimension. This is impractical for realistic deep learning tasks, where the representations are high dimensional. Neural entropic estimators tends to mitigate this shortage, but involves a lot of additional learnable parameters. On the other side, the recoverability loss estimation does not suffer from such disadvantage. By virtue of RKHS embedding with universal kernel we are able to compute the recoverability loss efficiently and without additional learnable parameters.

C Synthetic Data Experiments

If we extend the collection of continuous functions in \mathcal{C}_X (Section 3.1) to the measurable functions, and take as distance d the one induced from the L_2 norm on random variables, then the $Z \in \mathcal{C}_X$ that minimizes $\rho(Y|X)$ is almost everywhere equivalent to conditional expectation $\mathbb{E}[Y|X]$. Consequently, conditional expectation $\mathbb{E}[Y|X]$ can be used for testing $\rho(Y|X)$ values on synthetic data.

1D To demonstrate the ability of recoverability to capture the existence of a continuous map from one random variable to another, we use a simple 1D experiment. Let X be a normally distributed random variable, and let Z and W be defined as follows:

$$Z = f_1(X) = \text{sign}(X) \cdot X^2 \quad (\text{C.28})$$

$$W = f_2(X) = X^2. \quad (\text{C.29})$$

Since f_1 is invertible and f_2 is not, we can fully recover X from Z but not from W . Of course, we can fully recover Z and W from X , since we explicitly defined continuous maps f_1 and f_2 .

For this test we generated 1000 samples of X and estimated ρ^* with Theorem 1. The results are shown in Table C.1.

Theoretical recoverability loss for Table C.1

$$\mathbb{E}[Z|X] = Z \Rightarrow \rho(Z|X) = \sqrt{\mathbb{E}[(Z - \mathbb{E}[Z])^2]} = 0 \quad (\text{C.30})$$

$$\mathbb{E}[X|Z] = X \Rightarrow \rho(X|Z) = \sqrt{\mathbb{E}[(X - \mathbb{E}[X])^2]} = 0 \quad (\text{C.31})$$

$$\mathbb{E}[W|X] = W \Rightarrow \rho(W|X) = \sqrt{\mathbb{E}[(W - \mathbb{E}[W])^2]} = 0 \quad (\text{C.32})$$

$$\mathbb{E}[X|W = w] = \quad (\text{C.33})$$

$$= \mathbb{E}[\mathbb{1}_{X \geq 0} X|W = w] + \mathbb{E}[\mathbb{1}_{X < 0} X|W = w] = \quad (\text{C.34})$$

$$= \mathbb{E}[\mathbb{1}_{\sqrt{w} \geq 0} \sqrt{w}] + \mathbb{E}[\mathbb{1}_{-\sqrt{w} < 0} (-\sqrt{w})] = 0 \quad (\text{C.35})$$

$$\rho(X|W) = \sqrt{\mathbb{E}[(X - \mathbb{E}[X])^2]} = 1 \quad (\text{C.36})$$

100D Now, let X and N be 100-dimensional random vectors, with independent normally distributed entries, and Y be defined as

$$Y = \sum_{i \in [100]} (X_i + \alpha \cdot N_i), \quad (\text{C.37})$$

where α is some parameter. When α tends to zero, Y can be fully recovered from X , and when $|\alpha|$ is large, the noise N dominates the value of X , and consequently Y cannot be recovered from X . This behavior is visualized in Fig. C.1, where $\rho^*(Y|X)$, estimated on 1000 samples, is compared to its theoretical value.

Theoretical recoverability loss for Fig. C.1

$$\mathbb{E}[Y|X = x] = \sum_{i \in [100]} (x_i + \alpha \cdot N_i) = \sum_{i \in [100]} x_i \quad (\text{C.38})$$

$$\mathbb{E}[Y|X] = \sum_{i \in [100]} X_i \quad (\text{C.39})$$

$$\rho(Y|X) = \sqrt{\mathbb{E}[(Y - \mathbb{E}[Y|X])^2]} = |\alpha| \sqrt{100} \quad (\text{C.40})$$

	$\rho^* (\text{mean} \pm \text{std})$	ρ
$\rho^*(X Z)$	0.119 ± 0.004	0
$\rho^*(X W)$	0.974 ± 0.026	1
$\rho^*(Z X)$	0.099 ± 0.013	0
$\rho^*(W X)$	0.110 ± 0.019	0

Table C.1: The estimated distance from X to \mathcal{C}_W is larger than the distance from X to \mathcal{C}_Z , since we cannot fully recover X from W .

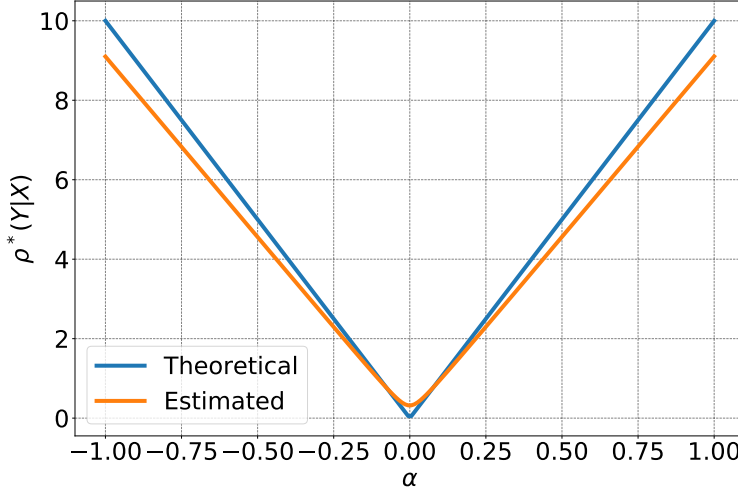


Figure C.1: Comparison between estimated $\rho^*(Y|X)$ and its theoretical value for different α .

Name	Nodes	Edges	Feat. dim.	Classes	Multilabel	Train	Val	Test	Directed
Reddit2 [Hamilton et al., 2017]	232,965	11,606,919	602	41	–	153,932	23,699	55,334	–
ogbn-arxiv [Hu et al., 2020]	169,343	1,166,243	128	40	–	90,941	29,799	48,603	✓
Flickr [Zeng et al., 2020]	89,250	449,878	500	7	–	44,625	22,312	22,313	–
PPI [Hamilton et al., 2017]	56,944	793,632	50	121	✓	44,906	6,514	5,524	–
ogbn-products [Hu et al., 2020]	2,449,029	61,859,140	100	47	–	196,615	39,323	2,213,091	–
PubMed [Yang et al., 2016]	19717	44324	500	3	–	60	500	1000	–

Table D.2: Dataset statistics.

D Dataset Statistics

The datasets used in our experiments are given in Table D.2.

E Embedding Types Used in Experiments on Real Data

- GraphConv:

$$x'_i = \Theta_1 x_i + \Theta_2 \sum_{j \in N(i)} e_{ji} x_j \quad (\text{E.41})$$

where Θ_1 and Θ_2 are trainable parameters.

- GCNConv:

$$x'_i = \Theta \sum_{j \in N(i) \cup \{i\}} \frac{e_{ji}}{\sqrt{\hat{d}_j \hat{d}_i}} x_j \quad (\text{E.42})$$

where $\hat{d}_i = 1 + \sum_{j \in N(i)} e_{ji}$, and Θ are trainable parameters.

- SAGEConv:

$$x'_i = W_1 x_i + W_2 \text{mean}_{j \in N(i)} \{x_j\} \quad (\text{E.43})$$

where W_1 and W_2 are trainable parameters.

- GINConv:

$$x'_i = h_\Theta \left((1 + \epsilon) x_i + \sum_{j \in N(i)} x_j \right) \quad (\text{E.44})$$

where h_Θ is an MLP and ϵ could be trainable.

- GATv2Conv:

$$x'_i = \alpha_{ii} \Theta x_i + \sum_{j \in N(i)} \alpha_{ij} \Theta x_j \quad (\text{E.45})$$

where:

$$\alpha_{ij} = \frac{\exp(a^T \text{LeakyReLU}(\Theta[x_i || x_j]))}{\sum_{k \in N(i) \cup \{i\}} \exp(a^T \text{LeakyReLU}(\Theta[x_i || x_k])))} \quad (\text{E.46})$$

and Θ are trainable parameters.

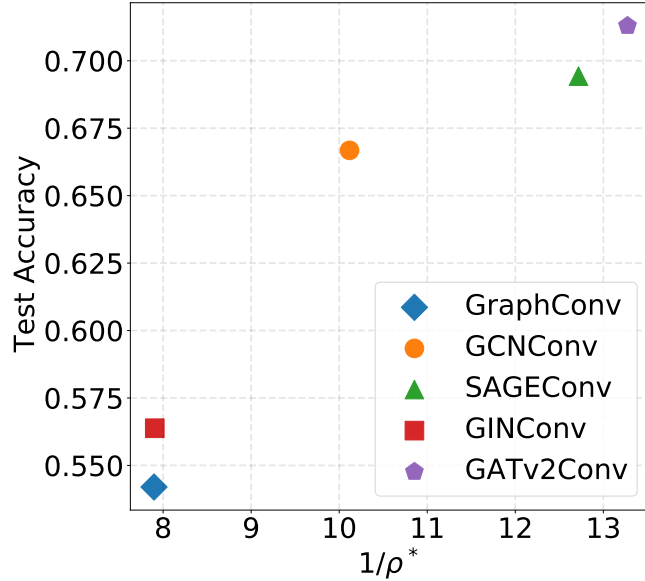


Figure F.2: The correlation between the test accuracy and the recoverability loss for ogbn-arxiv dataset.

F Additional Experimental Results

F.1 Correlation Between Recoverability and Aggregation Method Quality

Here we provide the results for ogbn-arxiv and ogbn-products datasets, Figs. F.2 and F.3, that are related to the experiment in Section 4.2.

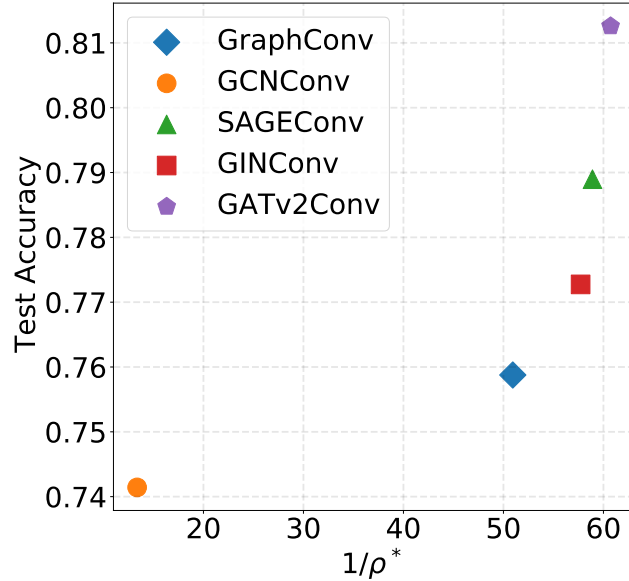


Figure F.3: The correlation between the test accuracy and the recoverability loss for ogbn-products dataset.

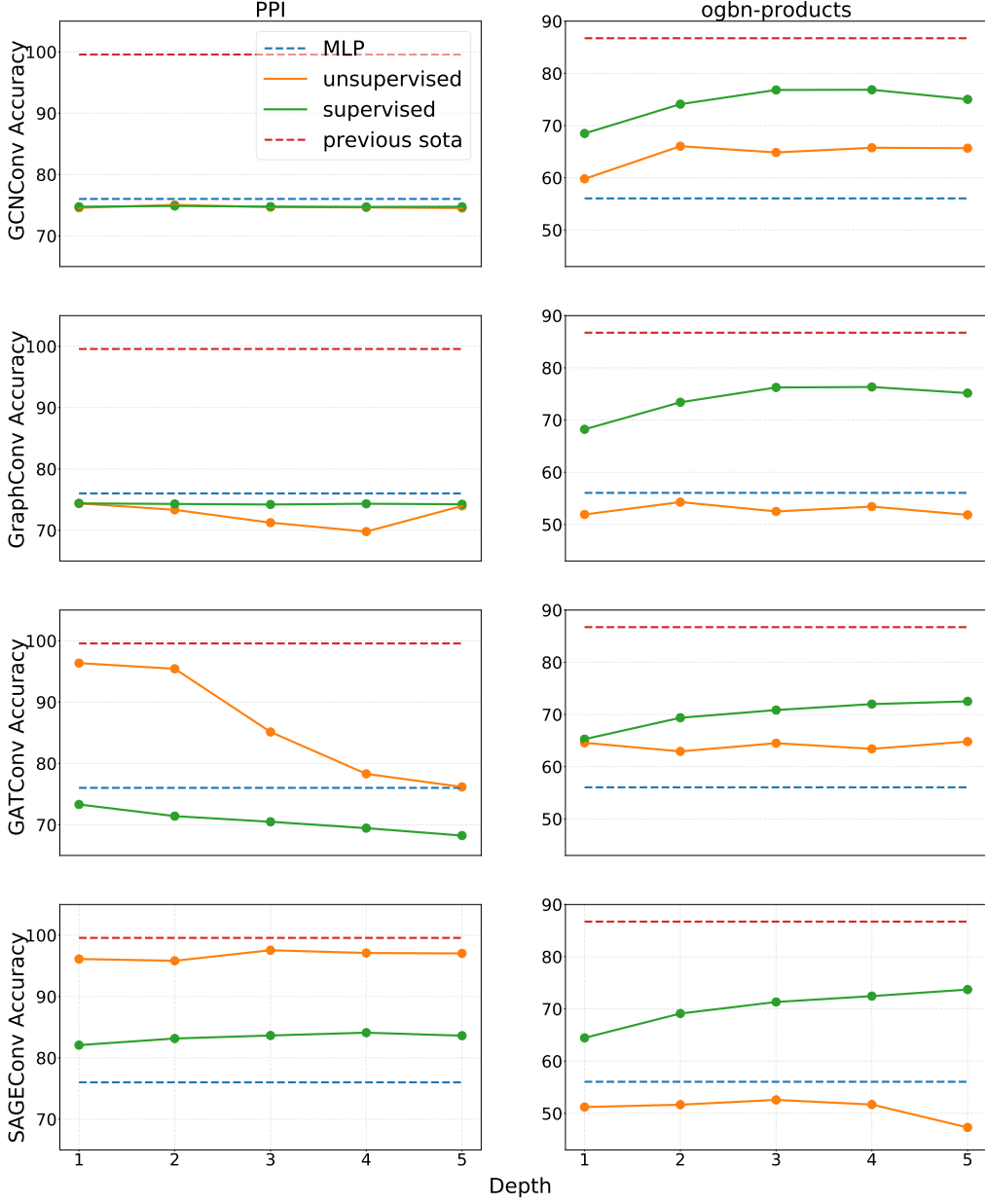


Figure F.4: GNN unsupervised learning using recoverability. Each column refers to different dataset. Each row corresponds to different graph convolution layer type. Each plot consists of test accuracy for supervised/unsupervised settings, MLP accuracy and previous supervised sota accuracy.

F.2 GNN Unsupervised Learning Using Recoverability

Here we demonstrate the results for PPI and ogbn-products datasets, Fig. F.4, that are related to the experiment in Section 4.5.

G Technical Notes

- There is a numerical instability in gradient computation of eigendecomposition $K = U\Lambda U^T$. The problem comes from equal eigenvalues in:

$$\frac{\partial L}{\partial K} = U \left\{ \left(\tilde{K}^T \circ \left(U^T \frac{\partial L}{\partial U} \right) \right) + \left(\frac{\partial L}{\partial \Lambda} \right)_{diag} \right\} U^T \quad (G.47)$$

where:

$$\tilde{K}_{ij} = \begin{cases} \frac{1}{\lambda_i - \lambda_j}, & i \neq j \\ 0, & i = j \end{cases} \quad (G.48)$$

and $(\cdot)_{diag}$ means all off-diagonal elements set to 0. To overcome this issue, we changed \tilde{K} to be:

$$\tilde{K}_{ij} = \begin{cases} \frac{1}{\lambda_i - \lambda_j}, & \lambda_i \neq \lambda_j \\ \frac{1}{\epsilon}, & \lambda_i = \lambda_j \\ 0, & i = j \end{cases} \quad (G.49)$$

- When we perform eigendecomposition, we do not have explicit zero eigenvalues. Thus instead of taking the first k non-zero eigenvalues, we simply clamp them between 0 and 1.